Chapter 3

Laser Guide Star Facility

3.1 Introduction

Adequately fine sampling of the wavefront by the wavefront sensor is required for optimal correction by the AO system. This requires a sufficient number of of photons to be detected within each subaperture. The need for a bright guide star close to the target star is therefore imperative [3].

Due to the unavailability of sufficiently bright natural guide stars (NGS) close enough to every target in the sky, AO systems cannot function in all directions of the sky. This poses a serious limitation to AO corrections. To overcome this limitation R. Foy and A. Labeyrie [33] suggested an alternative technique, - the creation of an artificial guide star in the sky using a laser; the Laser Guide Star (LGS) remains within the isoplanatic angle and inspite of some limitations, increases the sky coverage, thereby overcoming the restrictions set by the unavailability of a bright Natural Guide Star (NGS).

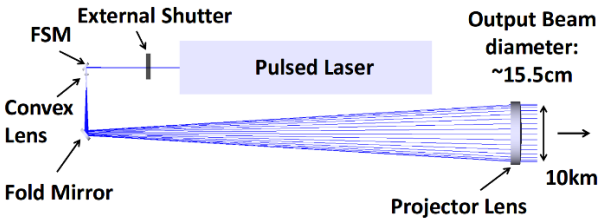

FIGURE 3.1: Optical layout of the laser projector.

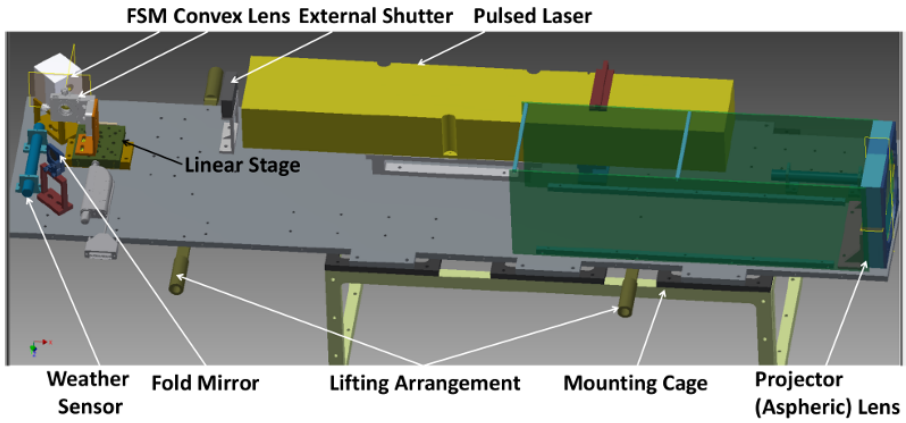

FIGURE 3.2: CAD Model of Laser projector.

iRobo-AO uses the Rayleigh back scattered light from an Ultraviolet (UV) LGS for wavefront correction. The brightness of the Rayleigh scattered guide stars depend on the density of the air molecules present at a given altitude and it falls exponentially with altitude. iRobo-AO Laser Guide Star Facility (LGSF) is optimized for a moderate height of 10 km above ground.

3.2 Description

The laser projector system is made of a pulsed UV laser, an external shutter, a fast steering mirror, a fold mirror, a convex lens and a plano-convex projector lens. The optical layout and mechanical CAD 3D design of the laser projection system are given in Fig. 3.1 and 3.2. Each component of laser projector system is briefly explained below. The specification of all the optics are given in Table 3.1.

The core of the laser projector system is a Q-switched Ultraviolet laser (10 Watt at 355 nm, with a pulse width of 33 ns and 10 kHz repetition rate) mounted in an enclosed projector assembly. A separate chiller is used to circulate cold water through the laser so that the laser diode working temperature is maintained at an optimum level.

As the laser is of type class IV[1], an additional external dielectric laser shutter is used to facilitate emergency shutdown independent of the internal laser shutter.

[1]It is the classification of laser safety class in the 'old system' of United states. The laser power more than 500 mW and non focused beam may cause severe, permanent damage to eye or skin, belongs to class IV.

Flexures and alignment errors of the components within the LGSF as well as its mounting structure could lead to an error in pointing of the LGS in the sky. The Fast Steering Mirror (FSM) (Fig. 3.3) is used to compensate for any mechanical pointing error so that all the subapertures on the deformable mirror are adequately illuminated. The FSM is a laser line UV coated at 350 nm and mounted on a tip-tilt stage with a maximum mechanical stroke of ±26 mradians which corresponds to ±1.89′ (in x direction) and ±1.3386′ (in y direction) in the sky.

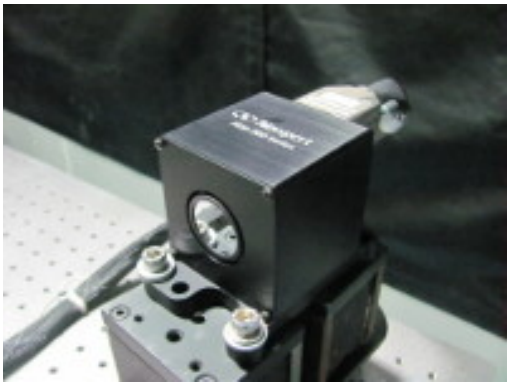

FIGURE 3.3: FSM.

An UV coated biconvex lens mounted on a linear actuator expands the laser beam to fill the entire projector lens. The stage is computer controlled and can be used to focus the LGS at the chosen altitude in the atmosphere.

A laser line mirror coated at 350 nm is then used to fold the beam towards the projector lens. The folded geometry using the FSM and the fold mirror makes the laser projector very compact.

The main projector lens is a plano-convex lens of diameter 165 mm and is custom made from UV grade Fused Silica, this lens is slightly aspheric and it focuses the output laser beam at a suitable height of about 10-12 km.

The complete assembly of the laser projector is shown in Fig. 3.4.

3.2.1 Optical Features

The optical performance of the design are discussed below.

The PSF of the laser projector optics is plotted in Fig. 3.5 from the Zemax FFT PSF cross-section generated data file. The angular FWHM of the LGS spot

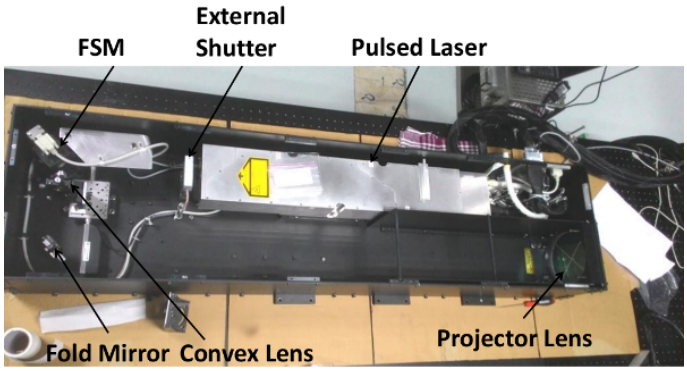

FIGURE 3.4: Laser projector assembly(Length:1.495 m, Width: 0.37 m, Height: 0.197 m, Weight: 65 Kg).

TABLE 3.1: Specification of Laser projector optics.

Name	Focal Length	Diameter	Material (UV-Grade)	ROC (mm)*	Center thickness
FSM Mirror and Fold Mirror (off the shelf)		25 mm,	Fused silica		
Convex lens (off the shelf)	15 mm	12.7 mm	Fused silica	±14.4 mm	5.9 mm
Projector Lens (custom made)	1.52769 m	165 mm	Corning HPFS grade 1A (C79-80)	Plano-Convex (727.39 mm) Conic constant: -0.58759	35 mm

* ROC: Radius of Curvature.

predicted by Zemax is 0.08787″. The seeing limited LGS width is 1.627″ [2] at λ=355 nm at 45^o zenith angle. The focused spot is seeing limited and does not depend on the design spot width as it is very small compared to the seeing. The focused spot width (FWHM) is the quadrature sum of both seeing and the design width, and the value is $\approx$ 1.63″.

In Fig. 3.6, the spot size is much smaller to Airy disc.

80% energy is encircled within the Airy Disc (Fig. 3.7).

[2]considering 1.2″ seeing at zenith at λ=0.55 μm; r_0: 7.6 cm at zenith: 45^0, at λ=0.55 μm (approx).

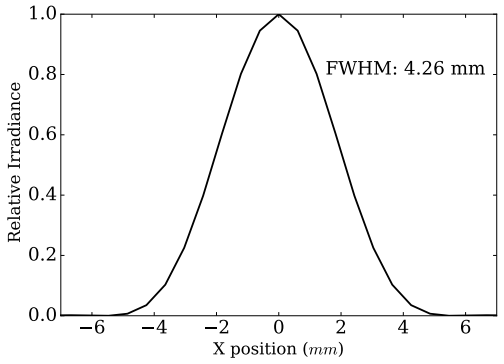

FIGURE 3.5: LGS PSF (Diffraction limited FWHM: 4.26 mm).

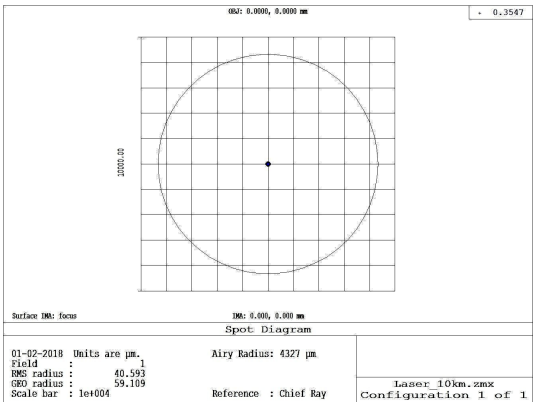

FIGURE 3.6: LGS Spot, well within the Airy Disc radius (4.327 mm).

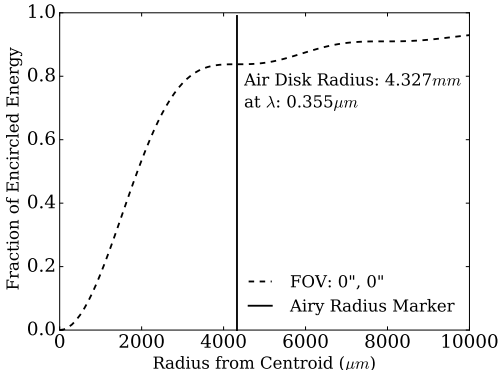

FIGURE 3.7: LGS Encircled Energy, 80% energy is encircled within the Airy Disc marked by the solid line.

3.3 Optical Integration

The optical integration of the laser projector was done within a laboratory of length around 25 m. In this section, the optical integration, including the focusing of the LGS is discussed.

3.3.1 Optical Alignment

The entire alignment process can be divided into three steps.

- **Alignment of the laser, FSM and the fold mirror (FM) without the Projector Lens (PL) and the convex lens (CL):** The laser is first mounted horizontally on the breadboard/base plate at the designed height

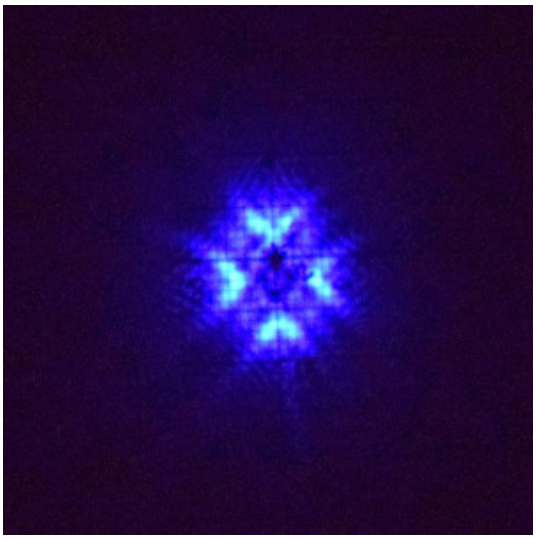

FIGURE 3.8: The shadow of the cross point of the threads at the PL mount when the light beam hits the PL through the aperture of the height gauge.

of 93 mm. The laser is operated in Continuous Wave (CW) mode, at low power (0.3 Watt) for the alignment purpose. It emits a pencil beam (waist diameter ($1/e^2$): 0.26 mm), the height of which with respect to the base plate is adjusted to the design value (93 mm). The center of the Projector Lens (PL) mount is spotted by using fine threads in crossed position across the diameter of the PL mount. It is very important that the laser is incident at the center of the PL (i.e. at the cross point of the threads) axially while maintaining the specified height. A height gauge with a 5 mm aperture at the said height of 93 mm is used to measure and achieve the specified height as per design, close to FSM, FM and PL mount. Then the laser pencil beam hits the cross point of the threads through the aperture of the height gauge to cast a shadow as depicted in Fig. 3.8. Tip-tilt adjustments of each component allows to ensure that the laser beam is centered on the following component.

- **Alignment of PL with FSM and FM:** The PL is mounted on a custom made lens holder and is aligned normal to the breadboard using a light back-reflection test. The reflected light from a plane mirror mounted on the PL mount is seen as a spot on the shutter aperture after back reflection from FM and FSM. The shutter is mounted close to the laser exit. A 0.5 mm thick shim below the PL holder is used to make the PL normal to the breadboard (Fig. 3.9).

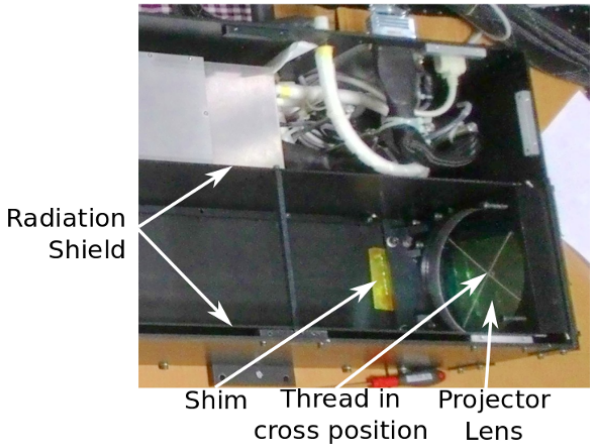

FIGURE 3.9: Cross thread arrangement in front of Projector Lens.

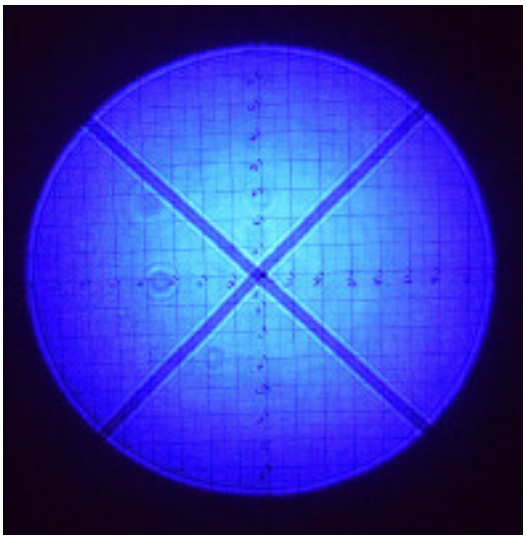

FIGURE 3.10: Uniformly Illuminated Laser Beam.

- **Alignment of Convex Lens (CL) with PL, FSM, FM:** After mounting the CL, it is ensured that the laser spot reflected from the FSM passes through the center of the CL at the entrance as well as exit surface. The focused spot is centred on the lens holder, and the elliptical laser spot is also at the centre of the FM. All these are achieved by adjusting the knobs of the CL mount in azimuth and X-Y direction. It is observed that the 160 mm diameter laser beam is uniformly illuminating a paper at a distance of 2 m and 22 m(Fig. 3.10) from the PL. It is to be noted that the beam is TEM_{00} mode. Uniform illumination indicates that the contours of equal brightness are circular, and it's center coincides with the PL center.

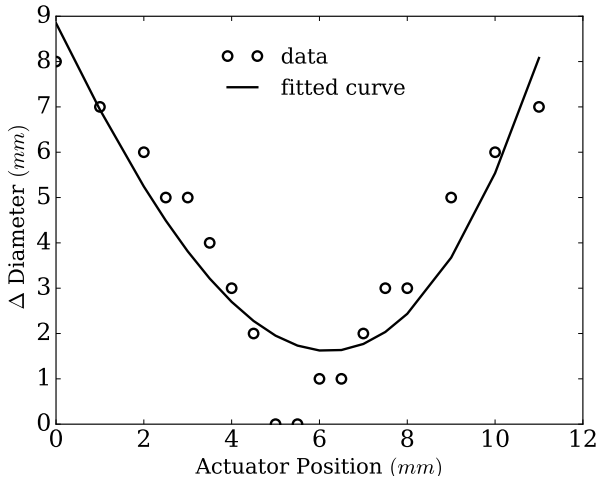

FIGURE 3.11: Beam diameter change across 22 meter for various actuator position.

3.3.2 Focusing Mechanism

It is extremely important that the LGS is well focused in the sky. To achieve this, the biconvex lens mounted on a high precision linear actuator in the laser projector is moved along the optical axis of the projector system. The position of the CL is set to different values and the diameter of the output beam from the projector lens is measured at different positions along the optical path across the available space of 22m. The difference in beam diameter across the separation is plotted for each CL position as shown in Fig. 3.11. The change in beam diameter is minimum for an actuator position of ∼6 mm. The seeing limited spot width of the LGS at an altitude of 10 km will be around 1.629″ at 0.355 μm wavelength. The cumulative degradation of the spot size is generated by the quadrature addition of the blurring of the LGS due to the defocusing and the seeing. An LGS width of up to ≈ 2″ (half of the subaperture at CCD39 WFS camera, Chapter 2-Wavefront Sensor) is within the acceptable range. The cumulative spot diameter of the LGS at 10 km due to the translation of the convex lens from the optimal position by the precession actuator is given the Fig. 3.12. The actuator has a stepping resolution 0.10 μm which is more than adequate to focus the LGS within the required spot size at 10 km.

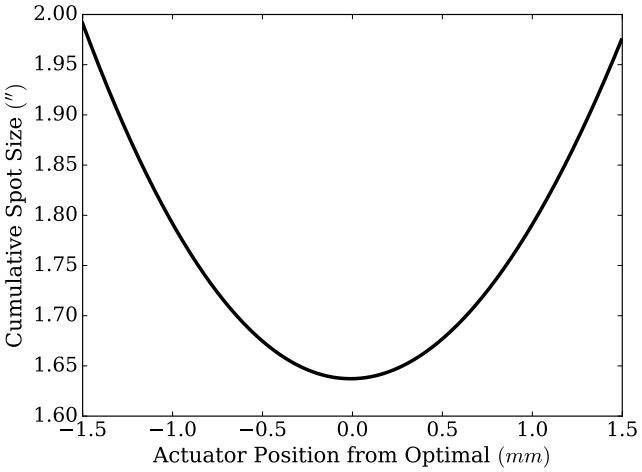

FIGURE 3.12: Cumulative effect on the LGS blurring considering both seeing and effects of various actuator positions as per Zemax.

3.3.3 Axial motion of the linear actuator along with the optic axis of the laser projector

The positions of the shadow of the thread in cross position (as mentioned in section 3.3.1 'Alignment of the laser, FSM and the fold mirror (FM) without the Projector Lens (PL) and the convex lens (CL)') due to the laser (in continuous wave mode), on a screen set at about 22 m away from the PL, for actuator position settings of 0 mm and 11 mm are noted. The measured shift of about 3 mm across 22 m corresponds to 28 arcseconds angular tilt.. Thus the laser beam deviates by 28 arcseconds for the motion of the linear actuator over its entire dynamic range. The FSM which has an angular stroke of ±113.4 arcseconds (in x direction) and ±80.316 arcseconds (in y direction) can easily compensate for this tilt.

3.4 Cooling Arrangement of Laser Diode

The efficiency, light output stability and the lifetime of the laser are very much sensitive to the laser diode temperature. As per specification sheet, the diode working temperature must be kept at 25.5°C ±0.2°C.

A water cooling arrangement is made using a chiller (placed at the telescope floor discussed later section) to maintain the temperature of the laser diode. There are two weather sensors to monitor the temperature and humidity inside the laser

projector. One of them is near the water panel of the laser projector and the second one is at the bottom of the box, near the Fold Mirror.

There is a pair of aluminium plate as a radiation shield to protect the laser body from the laser radiation inside the projector box, shown in Fig. 3.9.

3.5 Viewing geometry dependence on Laser beacons

As the subapertures move away from the projection axis of the laser, the spots appear more elongated. This situation has been discussed at length by several authors, e.g. [3, 87–89].

Here we compare two possibilities of laser projection geometries - projected from behind the secondary and from the side of the telescope; irrespective of the projection geometry some of the spots will appear elongated. A simulation was done to determine the radial elongation of the laser spots across various subapertures because of the viewing geometry, under the two cases.

3.5.1 Backscattered Photons

The first requirement in doing so is to estimate the number of backscatterd photons (n_p) from the LGS reaching per subaperture of the wavefront sensor. This was estimated following Hardy (1998) [3] and using the Lidar relation as in Equation 3.1 which was originally given by Gardner (1986) [90]. All the parameters used are given in Table 3.2 with their values and units. σ_B (m^2) is Effective backscatter cross-section and N(z)(m^{-3}) is number density of scatterers at range z. $\sigma_B N(z)$ for various z and wavelengths are presented in a tabular format in Hardy (1998)[3] and Δz typically varies from 100 to 400 meters [91–94].

$$n_p = \left(\frac{\lambda_B}{hc}\right) T_A^2 \frac{\sigma_B N(z)}{4\pi} \left(\frac{\Delta z}{z^2}\right) \left(E T_L d^2 T_0\right) \tag{3.1}$$

Using Equation (3.1) and Table 3.2 we get 34.639 photons/pulse/subaberture. Given a pulse width of 33 ns and and considering 1 msec. exposure we get about $\approx$ 346 photons per subaperture.

TABLE 3.2: Parameter and their values for estimating n_p.

Parameter	Value
Laser beacon wavelength, λ_B	0.355 μm
One-way transmission of atmosphere between - telescope and beacon (at 10 km and 45^o), T_A	0.36
Rayleigh Backscatter Parameter, $\sigma_B N(z)$ †	27.2 photons per million meters
Received range gate length, Δz	400 m
Range to the center of the range gate, z	10 km
Laser power	10 Watt
Pulse repetition rate	10^4 Hz
Pulse energy, E	10^{-3} Joule
Transmission of laser path to projection aperture, T_L	0.8855
Subaperture size at telescope entrance pupil, d	0.181 m
Transmission of laser path from primary - mirror to wavefront sensor, T_0	0.6025

† The product of the two parameters, $\sigma_B N(z)$ was obtained from Hardy (1998)[3]

3.5.2 LGS Elongation

Fig.3.13 shows the viewing geometry of the laser beacon. It can be seen that the elongation will progress in a radial direction from the laser projection axis. Considering an ideal situation where there is no elongation, we find that, the spot size diameter of a single lenslet of the lenslet array-SHWFS (refer wavefront sensor in Chapter 2) image on the wavefront sensor (WFS) camera to be 36 μm using Zemax FFT PSF cross section subroutine. Assuming the spot to be symmetric and Gaussian in nature, we equate this to $6\sigma_{org}$ (i.e.$\pm$ 3 σ_{org} range) cutoff, where σ_{org} is the standard deviation of the spot size without any elongation. For 24 μm pixel size of the camera we obtain

$$\sigma_{org} = 0.25 \quad \text{pixel} \tag{3.2}$$

The angular size of the elongation (Fig.3.13), β_{elo}, was estimated by [95], to be

$$\beta_{elo} \approx \left(\frac{\Delta z \times L}{z^2}\right)\left(\frac{206265 \times P_s}{24}\right) \quad \text{pixel} \tag{3.3}$$

where P_s, the plate scale on the WFS camera is $32.4\mu m/''$ and L is the distance of the subapertures (on the primary) from the laser launch point; the maximum

value of L for off-axis, and on axis, projections are 2 m and 1 m respectively in our case.

The standard deviation of this elongated spot, σ^*, again considering a Gaussian distribution (6 STD (i.e $\pm$ 3 STD) range) can be approximated to one-sixth of β_{elo} and the effective standard deviation of the elongated laser spot along the direction of elongation is given by

$$\sigma_{elo} = \sqrt{\sigma*^2 + \sigma_{org}^2} \quad \text{pixel} \tag{3.4}$$

The angular variation of the elongated spot at various subapertures can be estimated as follows. We define the laser projection coordinate as (x_{center}, y_{center}) with respect to the subaperture coordinate (x, y). The rotation angle of the spot is defined as

$$\gamma = \tan^{-1}\Big(\frac{y - y_{center}}{x - x_{center}}\Big) \tag{3.5}$$

The covariance matrix for a 2D Gaussian distribution whose major and minor axes are axially aligned to the frame of reference, can be written as,

$$COV_{matrix} = \begin{bmatrix} \sigma_{elo}^2 & 0 \\ 0 & \sigma_{org}^2 \end{bmatrix}$$

When the spot is rotated by γ the general covariance matrix can be rewritten as,

$$COV_{gen} = R(\gamma) COV_{matrix} R(\gamma)^T \tag{3.6}$$

$$COV_{gen} = \begin{bmatrix} a & b \\ c & d \end{bmatrix} \tag{3.7}$$

Where $R(\gamma)$ is rotator matrix,

$$R(\gamma) = \begin{bmatrix} \cos(\gamma) & -\sin(\gamma) \\ \sin(\gamma) & \cos(\gamma) \end{bmatrix} \tag{3.8}$$

and the covariance matrix elements are,

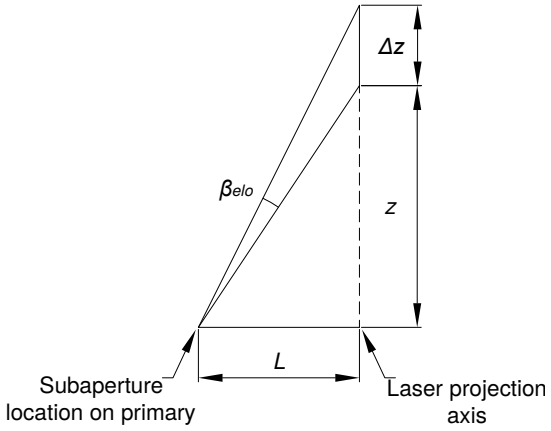

FIGURE 3.13: LGS elongation at a distance L from the laser projection axis.

$$
\begin{aligned}
a &= \sigma_{elo}^2 \cos^2\gamma + \sigma_{org}^2 \sin^2\gamma \\
b &= (\sigma_{elo}^2 - \sigma_{org}^2) \sin\gamma \cos\gamma \\
c &= b \\
d &= \sigma_{elo}^2 \sin^2\gamma + \sigma_{org}^2 \cos^2\gamma
\end{aligned}
$$

Using the Python random number generator routine "numpy.random.multivariate_normal(mean,COV_{gen},n_p)"[3] and equation (3.7), n_p photons are randomly distributed within each subaperture where the mean position of the distribution is the subaperture center. This was done for both the coaxial ($0 \leq L \leq 1$, $0 \leq \gamma \leq 2\pi$) and side ($0 \leq L \leq 2$, $0 \leq \gamma \leq \pi$) projection geometry.

The simulated results are presented in Figs. 3.14 and 3.15 where the red spot represents the laser projection axis and the square array represents a total of 11×11 subapertues. It can be seen that as we move outward from the point of projection the spots elongate radially and more so for the side projection geometry; the maximum elongation for coaxial and side projection was estimated to be $\sim 1.2''$ and $\sim 2''$ for our case. As discussed by Hardy (1998), [3] elongation of laser spots is a significant contributor to wavefront sensor measurement errors and also errors due to angular isoplanatism. In the iRobo-AO system, these errors for a side

[3]This Python routine draws n_p number of random samples from a multivariate normal distribution centred at "mean" and having generalised variance ("COVgen") with respect to an arbitrary axis.

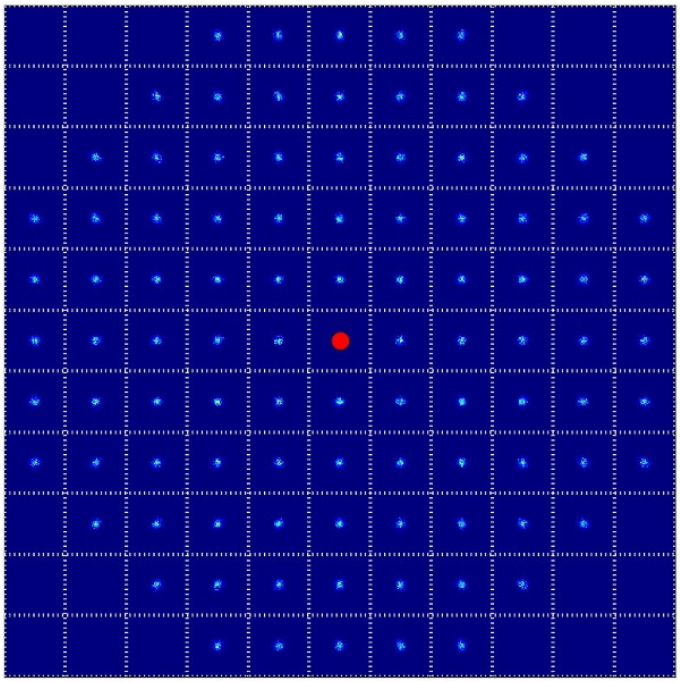

FIGURE 3.14: Array of LGS spots on each subaperture for coaxial laser projection (red spot is the projection axis).

projection geometry will be ≈ 1.67 times more than that for on-axis projection. Hence we have opted for on-axis laser projection.

3.5.3 Measurement Error

The expression for the standard deviation of the on-axis measurement error in Shack Hartmann sensors, in rms radians of phase difference per subaperture is given in Equation 2.11. Fried Parameter at zenith angle 45° at λ=0.355 μm is r_0=45 mm. FWHM of the spot (θ) is $\lambda/r_0 = 1.629''$. Using the parameters from Table 3.2, we get standard deviation of the on-axis measurement at λ=0.355 μm,

$$\sigma_\phi = \frac{26.992}{SNR}$$

SNR is the signal to noise voltage ratio of the detected signal (all quadrants). Voltage is proportional to incident photon (if there are other sources of noise then SNR will fall and integration is necessary over more than one pulse to get appropriate SNR). The 346 photons collected per sub-aperture from a 10 W laser

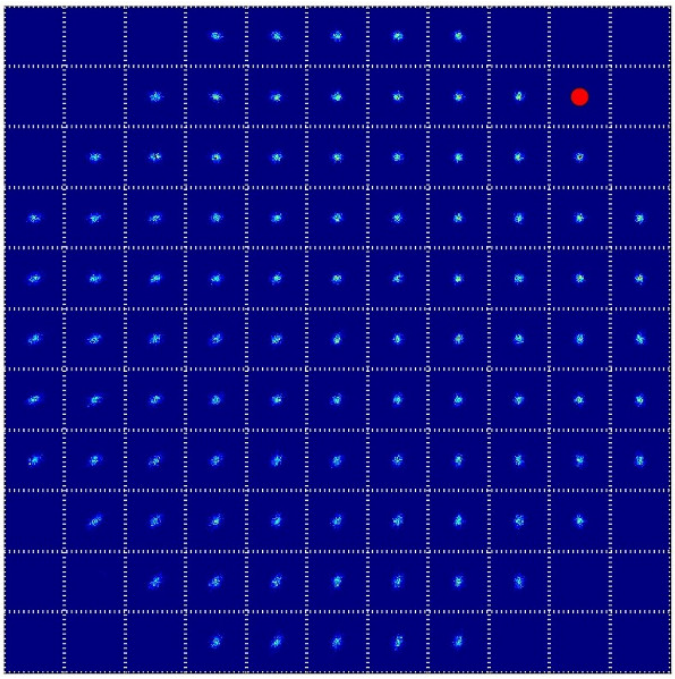

FIGURE 3.15: Array of LGS spots on each subaperture for laser projection from telescope side (red spot is the projection axis).

at 10 kHz at 355 nm in 1 msec exposure leads to photon SNR($\sqrt{346}$) of about 18.6. Thus,

$$\begin{aligned} \sigma_\phi &= \frac{26.992}{18.6} \\ &\approx 1.451\, radian \end{aligned} \tag{3.9}$$

3.6 Periscope

The laser projector is mounted on the side of the telescope as shown in the Fig. 3.16 and 3.17. The emanating beam is bend twice near the top of the telescope, so that the beam is launched into the sky from the back of the secondary mirror. The periscope system consists of two custom made 250 mm diameter laserline coated mirrors. One of the mirrors is mounted on the upper rim of the telescope just above the laser projector which reflects the laser light from the projector towards the second mirror mounted behind the cover at the back of the secondary mirror. With the help of the periscope the laser beam can be fired axially with respect to the telescope (Fig. 3.18). This is advantageous as explained in the section 3.5.2.

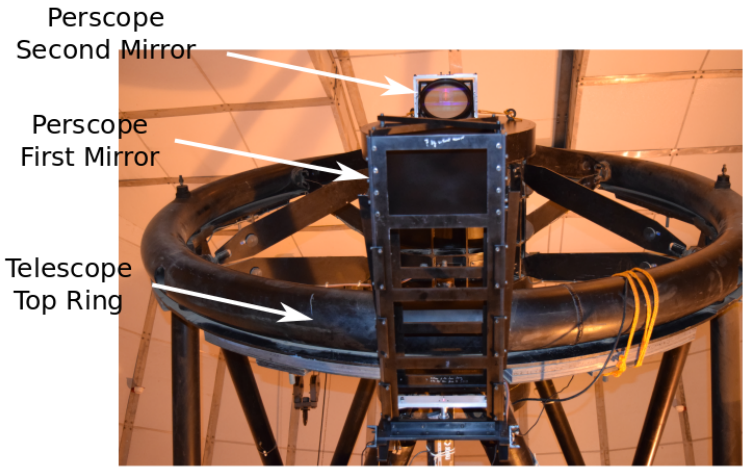

FIGURE 3.16: Periscope Mirrors.

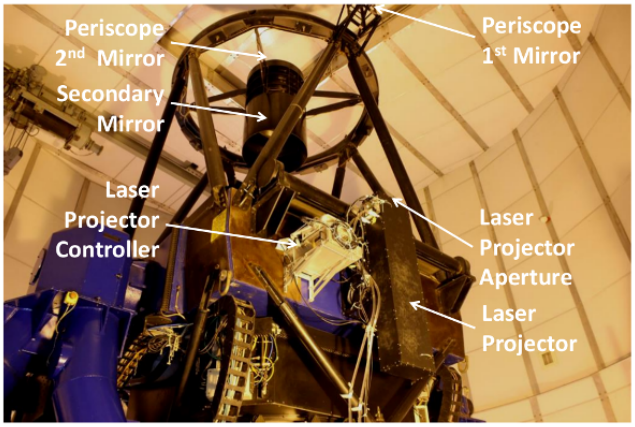

FIGURE 3.17: Laser projector mounted on telescope.

Fig. 3.19 shows the laser beam being test fired from IUCAA Girawali Observatory (IGO)- the photograph was taken with a U filter mounted in front of a modified DSLR camera.

3.6.1 Temperature Rise of First Periscope Mirror

The temperature of the first mirror of the periscope system can increase due to the laser heating. This can lead to expansion of the glass and the resultant stresses may lead to cracking of the mirror. The second mirror gets relatively lesser energy than the first mirror and gets more fresh air as it is much more exposed to the

FIGURE 3.18: LGSF test fired with periscope system from IGO.

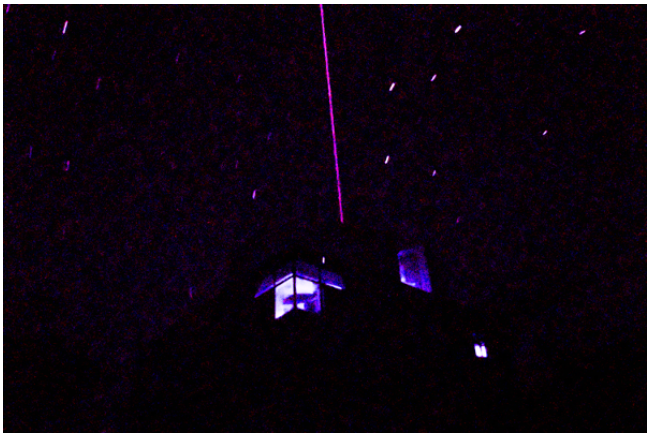

FIGURE 3.19: LGSF test fired from IGO.

TABLE 3.3: Periscope mirror parameters and their values for estimating temperature.

Parameter	Value	Parameter	Value
Absorption (a)	10%	Emisivity (ε)	0.9
Time Duration (t)	5 hour	Time Step (δt)	0.1 sec
Surrounding Temperature (T_s)	20^0C	Temperature at n^{th} step	T_n
Thickness (h)	2.5 cm	Radius (r)	12.5 cm
Mass (m)	3.068 Kg	Specific heat (s)	837 j/(Kg C)
Total Area of the body ($A=2\pi rh+2\pi r^2$)	1178 cm^2	Laser Power (w)	10 w

Note: Density (ρ): 2.5 gm/cc

sky. Thus if the first mirror survives, then there is no possibility of a crack in the second mirror.

The temperature rise of the first periscope mirror is calculated numerically. δt is the minimal time width over which the temperature rise increment is calculated. Let us consider at the n^{th} and $(n+1)^{th}$ iteration, the body temperature is T_n and T_{n+1} respectively. The surrounding temperature is T_s (say 20°C, average night temperature at IGO). The energy absorbed in the n^{th} step is $wa\delta t$, where w and a are the laser power and absorbtion. Internal thermal energy due to the body temperature is $ms(T_n - T_s)$. The Radiation loss at this stage is $\sigma\varepsilon A(T_n^4 - T_s^4)\delta t$. Thus the cumulative energy at n^{th} step is used for temperature increment for $n + 1^{th}$ iteration following the below equation.

$$\begin{aligned} ms(T_{n+1} - T_s) &= wa\delta t + ms(T_n - T_s) - \sigma\varepsilon A(T_n^4 - T_s^4)\delta t \\ T_{n+1} &= \frac{wa\delta t + msT_n - \sigma\varepsilon A(T_n^4 - T_s^4)\delta t}{ms} \end{aligned} \tag{3.10}$$

The temperature rise with time of the first periscope mirror due to the laser is calculated using Equation no. 3.10 and given in Fig. 3.20. The temperature increment is around ~ 1.5°C over a large period of 5 hours, which is very nominal. There is no chance of cracking due to thermal stress generated in it for such a small temperature rise.

3.7 Electronic Rack

The Laser projector controllers are mounted near the projector box on side of the telescope. Controllers of JDSU laser, FSM, external shutter (Fig. 3.21) are part of the laser projector controller assembly. The laser chiller produces vibration and hence it is placed on the telescope floor on a dampener to isolate its the vibration from the telescope.

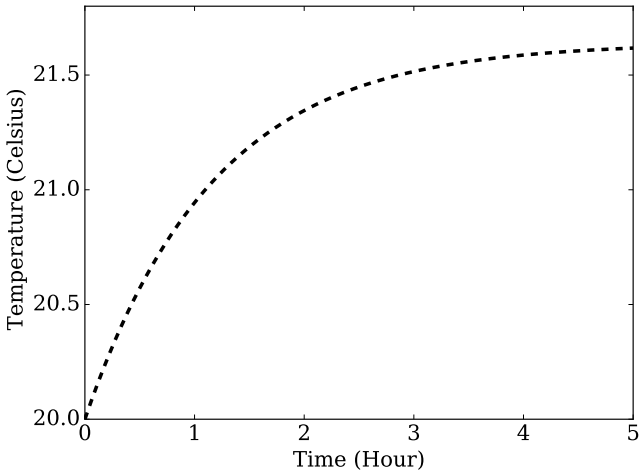

FIGURE 3.20: Temperature rise of the first mirror in the periscope vs time, $\sim 1.5°C$ temperature increment over a large period of 5 hours at 20°C ambient temperature.

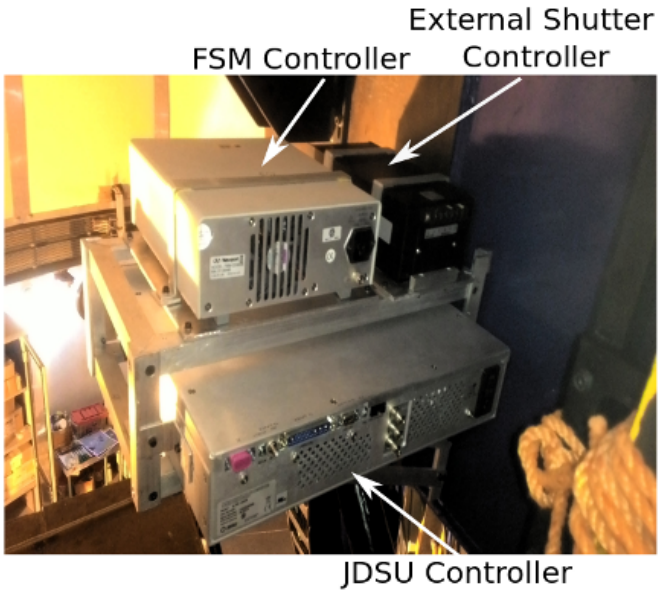

FIGURE 3.21: Laser projector controller, consists with JDSU, FSM, External Shutter controller.

3.7.1 Panel

There is a panel (Fig.3.22) on the laser projector box for the electrical connection of all the electronic components that are inside the projector assembly. The panel receives cables for the FSM, Weather Sensor, External Shutter, Linear Actuator, Laser's umbilical cord and Radio Frequency (RF) cable. There are also

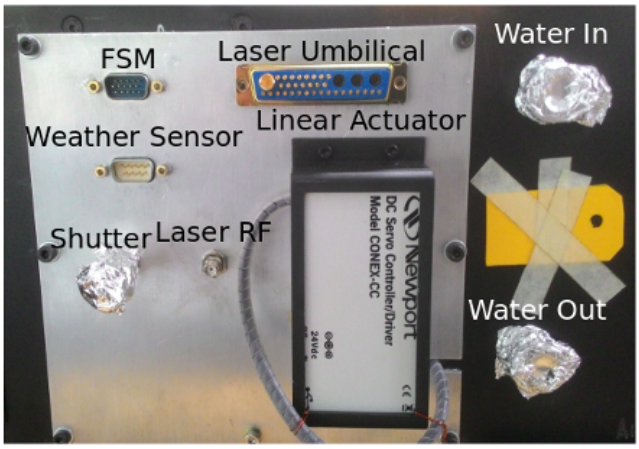

FIGURE 3.22: Panel of laser projector.

two plumbing connectors for the hot and cold water lines for cooling the UV laser.

3.7.2 Hanging Patch Cables

Several cables from the laser projector controller assembly which is mounted at the telescope side are connected with several components which are mounted at the telescope side ports as mentioned in the previous chapter 2 on the Cassegrain de-rotator. Cable routing from the laser projector to the Cassegrain side ports is tricky as it may entangle during telescope tracking. All these cables are routed through two permanent flexible cable racks through the Cassegrain de-rotator to avoid any entanglement and tear.

A pictorial representation of these cables is given in Fig. 3.23. For a more detailed description, please refer to Fig. 2.79 of Chapter 2.

3.7.3 Laser Cooling System

The chiller for the laser cooling system is heavy and bulky (Fig. 3.24). It is placed with dampener on the telescope floor instead of telescope side port or pier to avoid vibration on the telescope. The telescope can rotate in Azimuth from $-180°$ to $360°$. The chiller is kept in the middle position of the telescope Azimuth travel range, i.e. at Azimuth $90°$ for the equal rotations in both directions. A pictorial view of the chiller position on the telescope floor about the azimuth angle is given

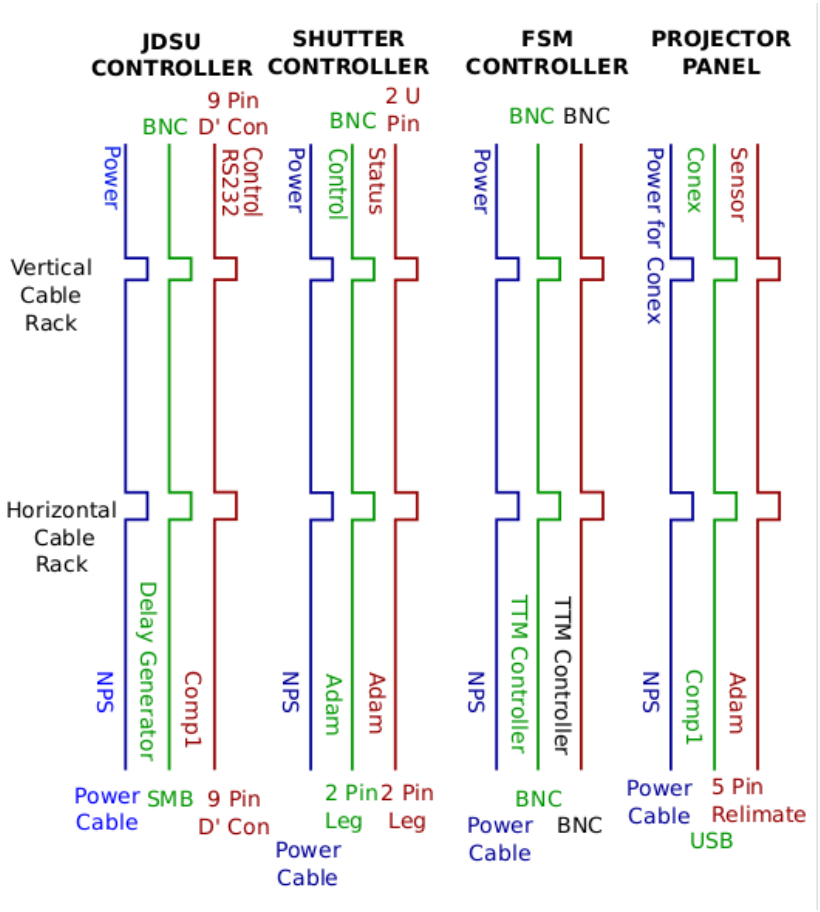

FIGURE 3.23: Laser Projector Patch Cables. The blue coloured lines represent power cables from electronic gadgets to the Network Power Switch (NPS). A BNC cable is connected from the laser projector to the Delay Generator with SMB connector for Range gating, pulse electronic signal. A RS232 cable is connected to Computer1 (Comp1) to operate the laser. A BNS-2pin leg and 2 U type pin-2 pin leg attached cables are connected with the ADAM module for controlling the shutter and reading the shutter status respectively. 2 BNC cables are connected to the four-channel TTM controller for the FSM mirror. A USB cable (for laser Conex) is connected with Comp1 for the LGS focussing linear stage. A cable with 5 pin Relimate connector is attached with the ADAM module for the weather sensors inside the laser projector.

in Fig. 3.25. A precaution for free movement without entangling of the water pipes hanging from the laser projector to the chiller is taken care.

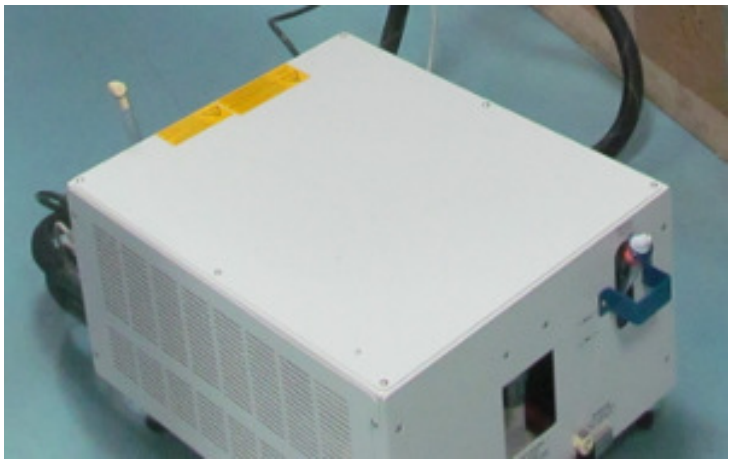

FIGURE 3.24: Laser Chiller.

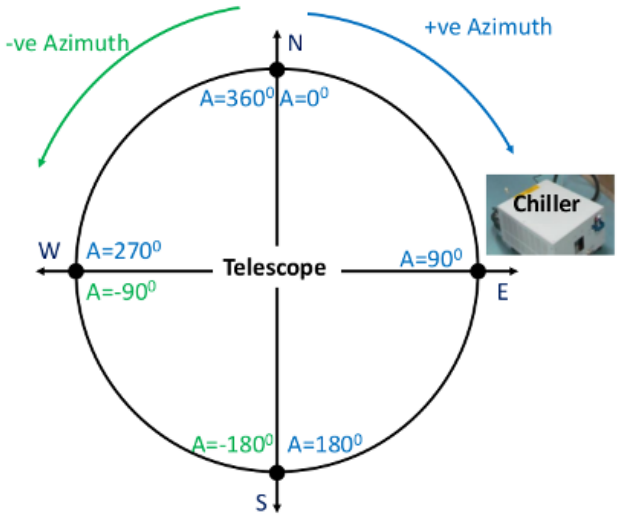

FIGURE 3.25: Position of chiller at dome floor.

Pump Capacity The height of the Laser projector from the telescope floor is around 4.5 m. The water pressure at the said height is P=4.5 m× 997 Kg/m^3× 9.81 m/s^2 ≈0.44 bar. The coolant flow rate requirement is < 2 liter per minute at 1 bar. As the pressure at the chiller is only 0.44 bar, which is well within the pressure overhead limit value of the chiller, it can maintain the required coolant flow.